Electronic Supplementary Material (ESI) for Dalton Transactions
This journal is © The Royal Society of Chemistry 2014

Supporting information

Tetrahedral Tetrazolate Frameworks For high H_2 and CO_2 Uptake

Fei Wang, Duan-Chuan Hou, Hui Yang, Yao Kang, Jian Zhang *

State Key Laboratory of Structural Chemistry, Fujian Institute of Research on the Structure of Matter, the Chinese Academy of Sciences, Fuzhou, Fujian 350002, P. R. China.

E-mail: zhj@fjirsm.ac.cn

This journal is © The Royal Society of Chemistry 2014

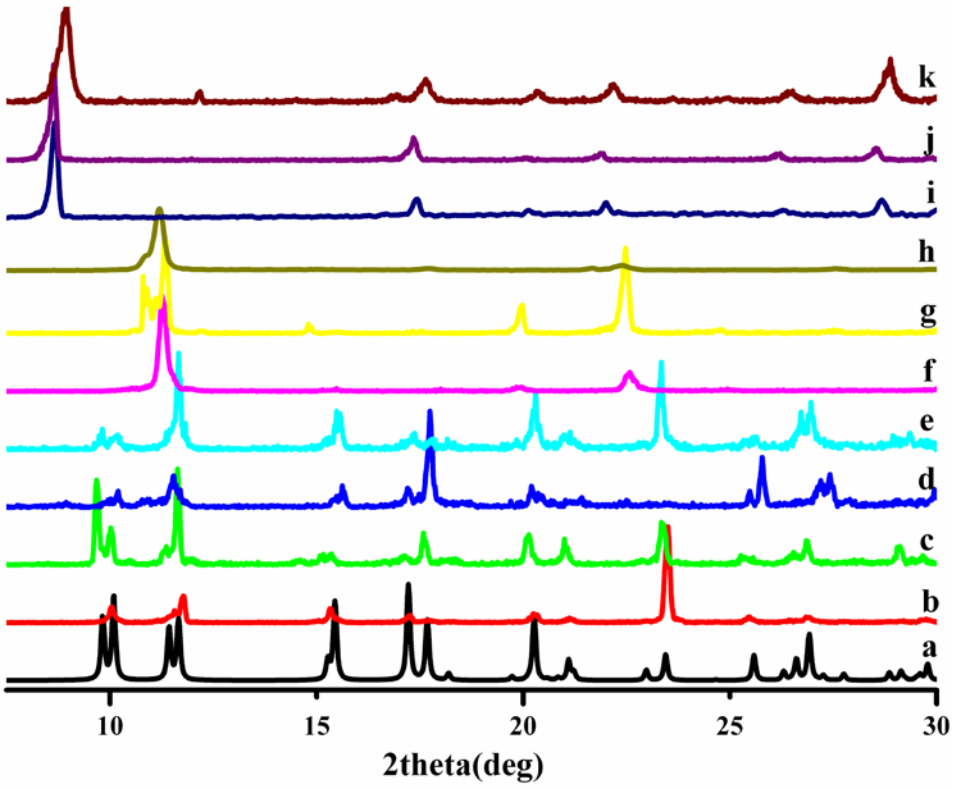

Fig.S1 The powder XRD patterns of **1** to **3** under different conditions.(a) simulated **1**; (b) **1** soaked in ether; (c) **1** soaked in tetrahydrofuran (THF); (d) **1** soaked in toluene; (e) **1** soaked in ethanol; (f) **1** soaked in acetone; (g) **1** soaked in CH_2Cl_2; (h) **1** after degassed; (i) **1** soaked in methanol under room temperature; (j) **3** soaked in methanol under room temperature; (k) **3** soaked in methanol under room temperature.

As shown in fig. s1, compound **1** shows high chemical-stability in common solvents with low boiling points, such as acetone, ether, CH_2Cl_2 or ethanol, except methanol.

This journal is © The Royal Society of Chemistry 2014

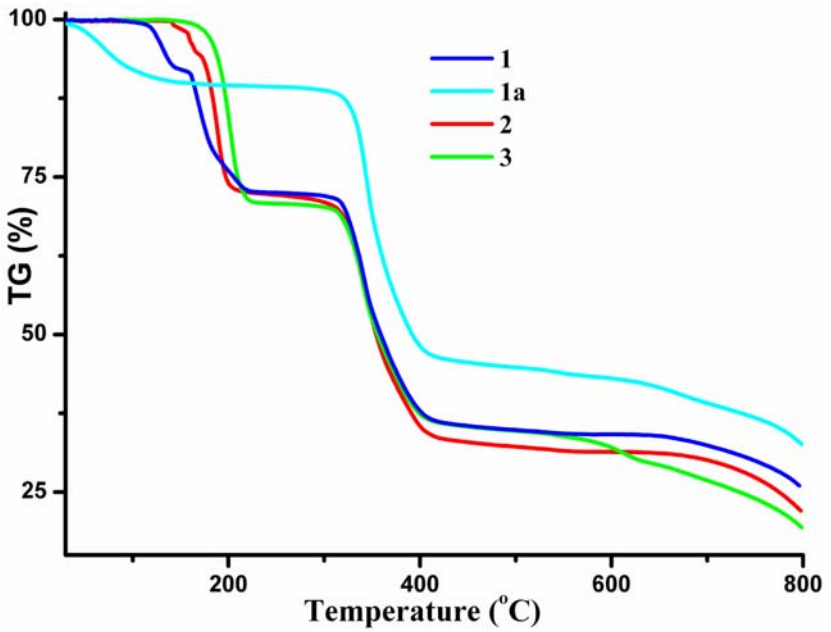

Fig. S2. The TG plots of **1** to **3**.

The photoluminescence properties of **1** to **3** have been explored at room temperature in the solid state (Fig. s3). Compounds **1** to **3** display blue emission band with peak maximum at 410, 414 and 436 nm (excitation at 340 nm), respectively. According to the previous reports about the Zn(II)-carboxyl metal-organic frameworks, the emission is tentatively assigned as originating from the ligand-to-metal charge-transfer (LMCT).

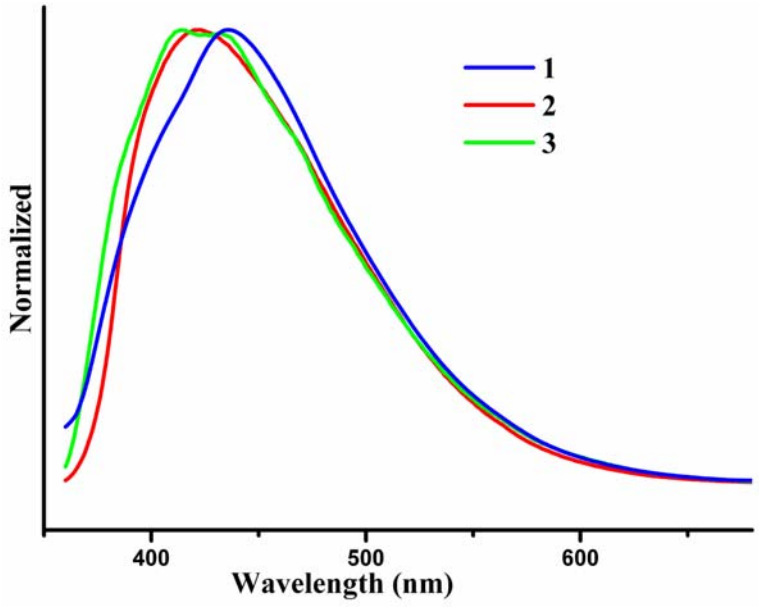

Fig.S3 The solid-state emission spectra of **1** to **3** at room temperature.

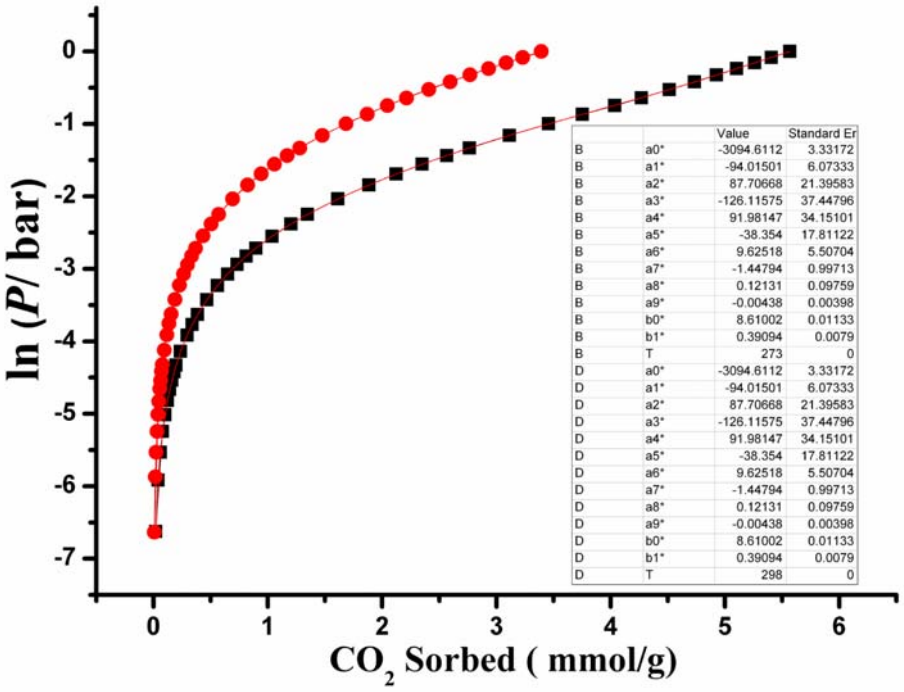

		Value	Standard Er
B	a0*	-3094.6112	3.33172
B	a1*	-94.01501	6.07333
B	a2*	87.70668	21.39583
B	a3*	-126.11575	37.44796
B	a4*	91.98147	34.15101
B	a5*	-38.354	17.81122
B	a6*	9.62518	5.50704
B	a7*	-1.44794	0.99713
B	a8*	0.12131	0.09759
B	a9*	-0.00438	0.00398
B	b0*	8.61002	0.01133
B	b1*	0.39094	0.0079
B	T	273	0
D	a0*	-3094.6112	3.33172
D	a1*	-94.01501	6.07333
D	a2*	87.70668	21.39583
D	a3*	-126.11575	37.44796
D	a4*	91.98147	34.15101
D	a5*	-38.354	17.81122
D	a6*	9.62518	5.50704
D	a7*	-1.44794	0.99713
D	a8*	0.12131	0.09759
D	a9*	-0.00438	0.00398
D	b0*	8.61002	0.01133
D	b1*	0.39094	0.0079
D	T	298	0

Fig. S4. Virial analysis of the CO_2 sorption data for **1a**.

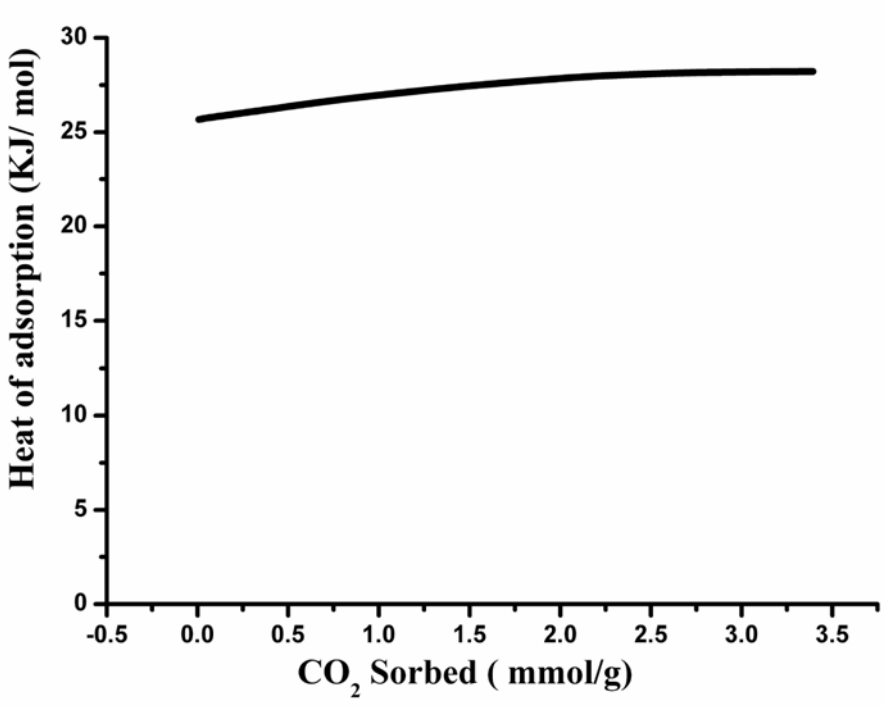

Fig. S5. Heat of CO_2 adsorption for **1a** estimated by the virial equation.

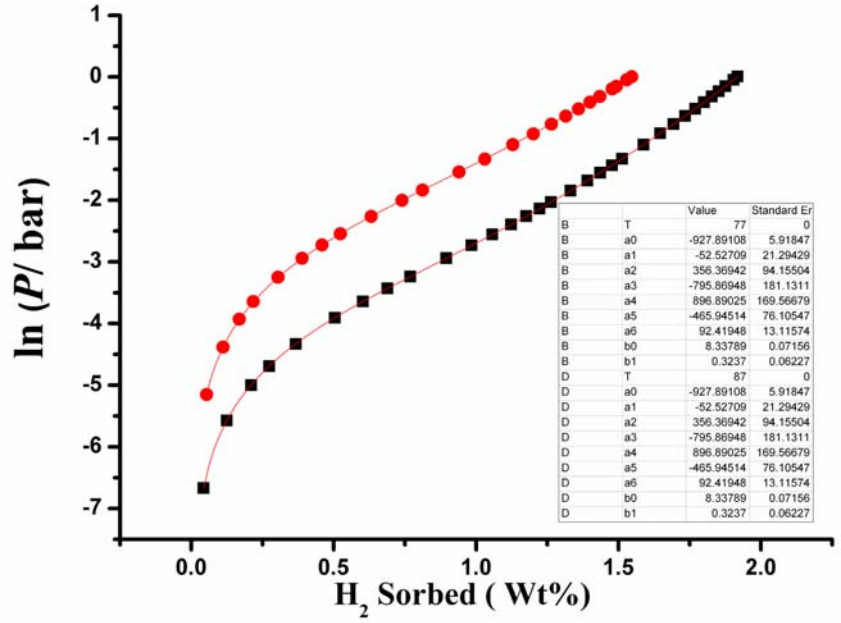

		Value	Standard Er
B	T	77	0
B	a0	-927.89108	5.91847
B	a1	-52.52709	21.29429
B	a2	356.36942	94.15504
B	a3	-795.86948	181.1311
B	a4	896.89025	169.56679
B	a5	-465.94514	76.10547
B	a6	92.41948	13.11574
B	b0	8.33789	0.07156
B	b1	0.3237	0.06227
D	T	87	0
D	a0	-927.89108	5.91847
D	a1	-52.52709	21.29429
D	a2	356.36942	94.15504
D	a3	-795.86948	181.1311
D	a4	896.89025	169.56679
D	a5	-465.94514	76.10547
D	a6	92.41948	13.11574
D	b0	8.33789	0.07156
D	b1	0.3237	0.06227

Fig. S6. Virial analysis of the H_2 sorption data for **1a**.

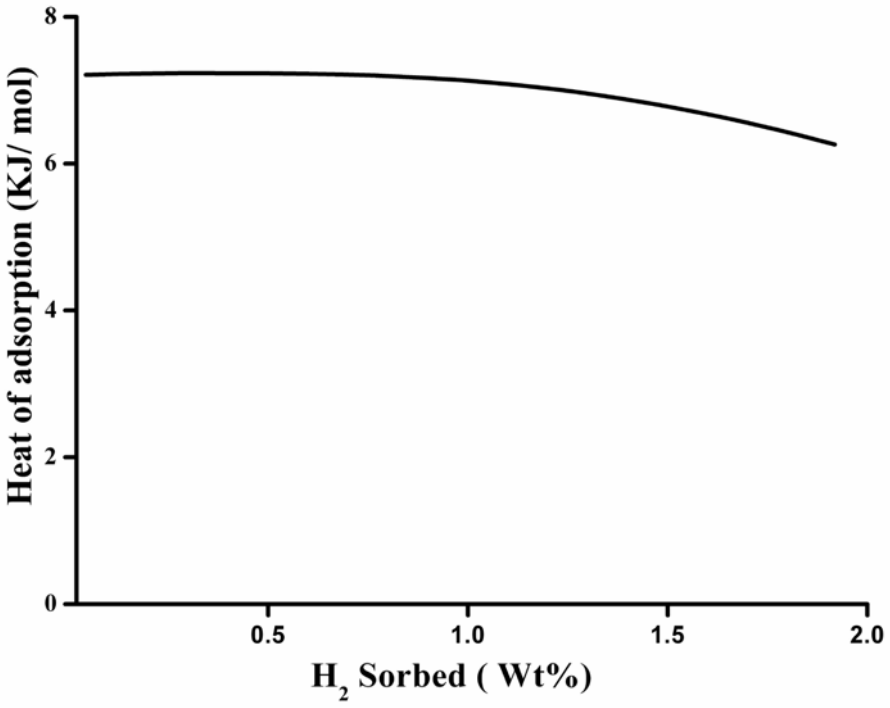

Fig. S7. Heat of H_2 adsorption for **1a** estimated by the virial equation.

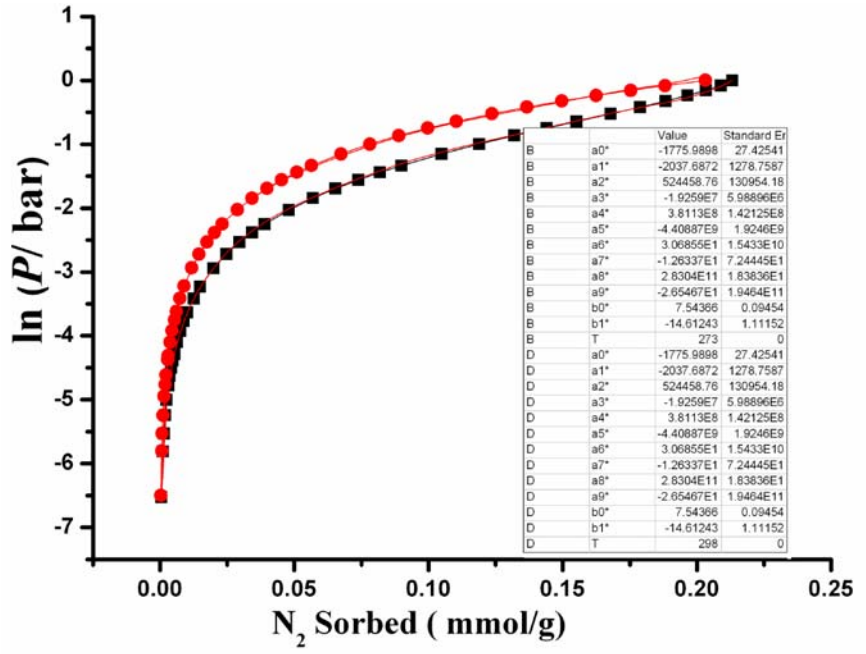

Fig. S8. Virial analysis of the N_2 sorption data for **1a**.

Table S1. Adsorption data and isosteric heat data for **1a**.

BET (Surface area, m^2/g)	792
Vp (the measured pore volume, cm^3/g)	0.39
CO_2 Adsorptive amount (mmol/g) at 273K	5.57
CO_2 Adsorptive amount (mmol/g) at 298K	3.42
Qst(CO_2) (Isosteric heat of adsorption at 1 atm, kJ/mol)	25.68
H_2 Adsorptive amount (mmol/g) at 77K	9.6
H_2 Adsorptive amount (mmol/g) at 87K	7.7
Qst(H_2) (Isosteric heat of adsorption at 1 atm, kJ/mol)	7.22
fH_2(%) (The fraction of the pore volume filled by liquid H_2 (ρH2 =0.0708 g/cm^{-3}) at 1 atm and 77 K)	69.5